State-of-the-Art in the Design and Manufacture of Low Acceleration Sensitivity Resonators

R.B. Haskell[1], J.E. Buchanan[2], P.E. Morley[1], B.B. Desai[2], M.A. Esmiol[1], M.E. Martin[2], and D.S. Stevens[1]

[1]Vectron International-Hudson, 267 Lowell Rd., Hudson, NH 03051
[2]Vectron International-CINOX, 4914 Gray Road, Cincinnati, OH 45232

*Abstrac*t – **This paper reviews the design and manufacture of an improved Quad Relief Mount (QRM) resonator. It discusses the mechanical resonance and how the lead-frame structure was modified to push the mechanical resonance well above 2kHz. The results of a Design of Experiments (DOE) are discussed and show that the azimuthal mounting angle (Ψ) has a dramatic effect on the g-sensitivity performance of the QRM resonator. Finally, preliminary results on a QRM design that uses a larger diameter blank (0.390") are compared to the current 0.320" QRM design.**

***Keywords* – acceleration, sensitivity, g-sensitivity, vibration, quartz, crystal, resonator, QRM**

I. Introduction

It is well known that low values of acceleration sensitivity can be achieved by utilizing a symmetric mounting structure that is well aligned with the acoustic mode center. Theoretical works by Tiersten and Zhou showed that for a plano-convex resonator with perfectly aligned acoustic mode and symmetric support centers, the effect of the intrinsic asymmetry due to the contour is a few parts in 10^{12} per g for the in-plane acceleration sensitivity. They also showed that the normal acceleration sensitivity increases linearly with offset of the centers [1-3].

Creating a symmetric mounting structure is possible, but maintaining a symmetric stress field with respect to the symmetric mounting structure has proven to be difficult to achieve. In reality, residual stresses caused by annealing of the clips, shrinkage or expansion of the adhesive, and manufacturing imperfections will alter the distribution and symmetry of the applied stress field. Because the applied stress may no longer be aligned with respect to the acoustic mode, there is an effective asymmetry that will result in greater acceleration sensitivity.

Recently, work done by Haskell et al. has demonstrated a new four-point mounting structure with built in residual static stress relief and good in-plane symmetry [4-5]. The structure minimized the effects of residual static stresses which resulted in reproducibly low values of observed acceleration sensitivity (mid parts in 10^{11} to low parts in 10^{10}).

The work presented in this paper reviews the design and manufacture of an improved design. In addition, it discusses the mechanical resonances and how the lead-frame structure was modified to push the mechanical resonance well above 2kHz. The results of a Design of Experiments (DOE) are discussed and show that the azimuthal mounting angle (Ψ) has a dramatic effect on the g-sensitivity performance of the QRM resonator. Finally, preliminary results on a QRM design that uses a larger diameter blank (0.390") are compared to the current 0.320" QRM design.

II. Acceleration Sensitivity Measurement

For all the work described here, passive measurements were made without the use of an oscillator circuit [6-7]. The method uses an HP4396B network/spectrum analyzer combined with a frequency source which we will refer to as the network analyzer method.

The acceleration sensitivity measurements were obtained by measuring along three mutually perpendicular axes. For the previous and new designs, the acceleration sensitivity was measured as shown in Fig. 1. The acceleration sensitivity components are denoted by Γx, Γy, and Γz.

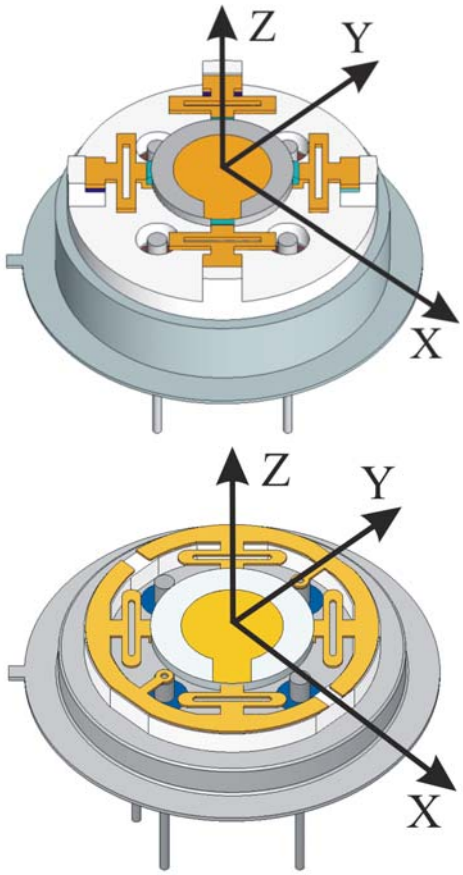

Fig. 1. Axial convention for the acceleration measurements.

III. Improvements In The QRM Resonator

A. The Old and New QRM Designs

The layout of the old QRM resonator structure is shown in Fig. 2. It consists of a machinable ceramic base, a chemically etched lead-frame, and a quartz blank. The lead-frame is made of 0.004" thick ½ hard nickel-silver (CTE ~ 16.4 ppm/°C) and it is formed to have support shelves that align and hold the crystal. The depth of the form controls the alignment of the crystal and lead-frame mid-planes.

The ceramic base provides a rigid, coplanar set of four points on which the lead-frame assembly can be mounted using a non-conductive adhesive. Once the adhesive cures, the unused portions of the lead-frame are cut away leaving the QRM support structure shown. The crystal blank is then placed onto the formed supports using a conductive adhesive for support and electrical connections. The electrical connections are completed by using 0.004" gold wire to the package pins.

The layout of the new QRM resonator structure is shown in Fig. 3. It consists of a low profile HC40 header, a laser cut ceramic ring with four alignment flats, and a chemically etched Kovar (CTE ~ 5.87 ppm/°C) lead-frame with increased surface area and built-in electrical connections. The features of the new design are similar to the old design (i.e. formed support shelves, rigid ceramic support, and mid-plane alignment), but the new design uses a set of Kovar assembly fixtures (Figs. 4 and 5) to align the QRM components precisely while curing.

Fig. 2. Old 8mm (0.315") QRM resonator structure.

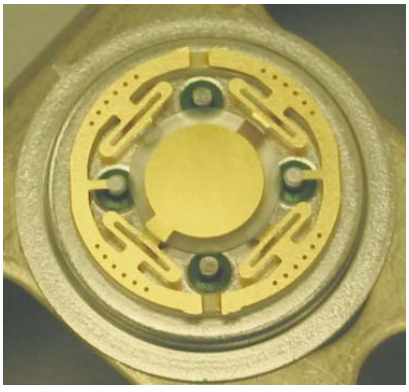

Fig. 3. New 0.320" QRM resonator structure.

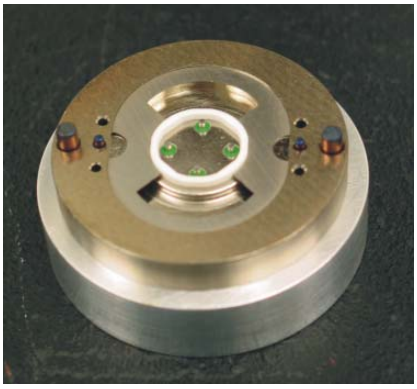

Fig. 4. Kovar assembly fixture (alignment of the ceramic ring).

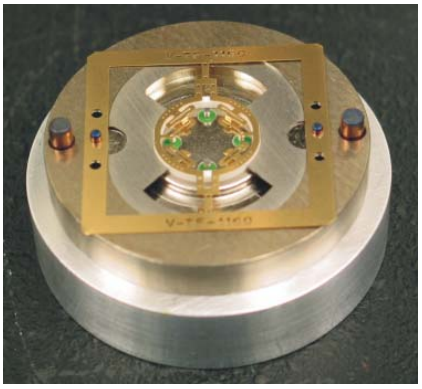

Fig. 5. Kovar assembly fixture (alignment of the lead-frame).

B. Mechanical Resonance of the Old QRM Resonator

A mechanical resonance in the range of 1.5 to 1.9 kHz was observed for the old QRM resonator structure and FEA predicted that increasing the lead-frame thickness from 0.004" to 0.006" would push the resonance from 1.9 to 3.8kHz for the ½ hard nickel-silver lead-frame material. Using a stiffer Kovar lead-frame material, the new QRM design was built using 0.004" and 0.006" thick lead-frames and tested for mechanical resonances up to 2.5kHz (Figs. 6 and 7). As can be seen, the mechanical resonance is at 2.3kHz for the 0.004" Kovar lead-frame, while the resonance is off the scale for the 0.006" lead-frame.

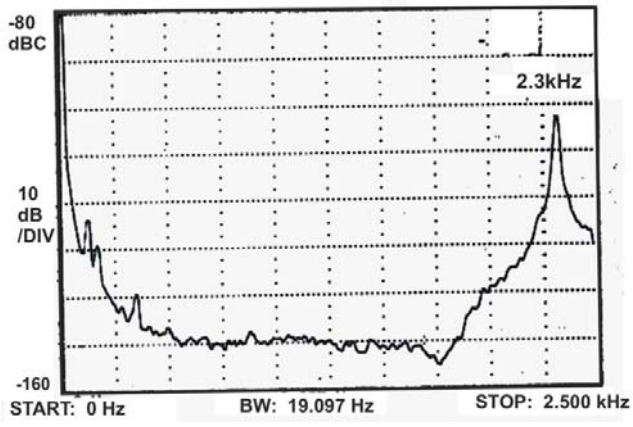

Fig. 6. Mechanical resonance for the 0.004" Kovar lead-frame (new QRM).

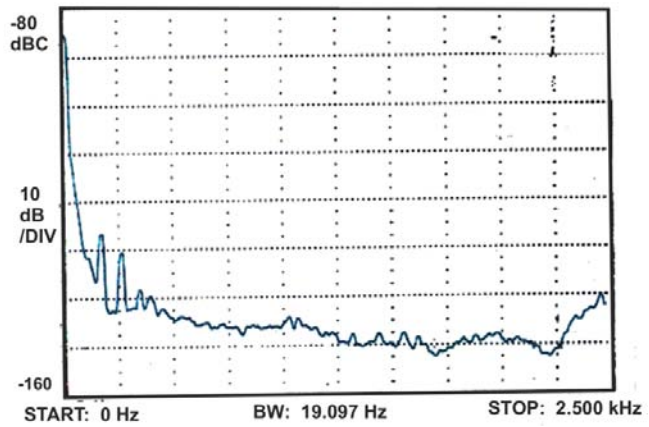

Fig. 7. Mechanical resonance for the 0.006" Kovar lead-frame (new QRM).

C. G-Sensitivity of the Old and New QRM Designs

The crystal blank design parameters are listed in Table I for the old and new QRM designs. Typical total Γ g-sensitivity results are shown in Fig. 8. The new design with a ϕ = 22° has an average total Γ of 1.59 x 10^{-10} per g compared to a total Γ of 1.85 x 10^{-10} per g for the old QRM design. The new design with a ϕ = 23° is slightly higher for total Γ at 2.11 x 10^{-10} per g. However, for both the ϕ = 22 and 23° new QRM designs, the standard deviations are much lower than the old QRM standard deviation (0.43 x 10^{-10} per g and 0.50 x 10^{-10} per g compared to 0.85 x 10^{-10} per g).

TABLE I
CRYSTAL BLANK DESIGNS FOR THE OLD AND NEW QRM STRUCTURES

QRM version	Plano-convex 10MHz 3rd overtone			
	ϕ angle (°)	Ψ angle (°)	Contour (diopter)	Electrode Dia./Material
Old QRM 0.315" (no flats)	22	random	4.0	0.209" Cr/Au
New QRM 0.320" (-x flat)	22	-20	1.5	0.250" Cr/Au
New QRM 0.320" (-x flat)	23	-20	1.5	0.250" Cr/Au

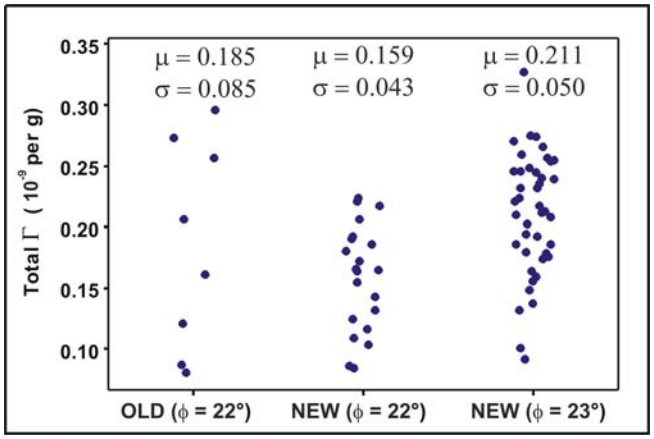

Fig. 8. Typical g-sensitivity results for the old and new QRM resonators.

IV. The Effects Of Contour And Ψ Angle

A. Design of Experiments (DOE) Settings

A DOE was planned for our ϕ = 23° QRM structure to better understand the impact of design settings on g-sensitivity and crystal parameters. The design settings (Table II) were set to explore 2 factors, contour and Ψ mounting angle, with 3 levels for each factor resulting in a total of 9 different combinations of settings. Ten replicates were built for each combination for a total of 90 10MHz 0.320" QRMs.

TABLE II
DOE DESIGN SETTINGS

Group	Plano-convex 10MHz 3rd overtone 4 flats		
	Ψ angle (°)	Contour (diopter)	θ angle (°)
1	-20	1.5	33° 59' 50"
2	-20	2.5	33° 59' 40"
3	-20	4.0	33° 59' 30"
4	0	1.5	33° 59' 50"
5	0	2.5	33° 59' 40"
6	0	4.0	33° 59' 30"
7	+20	1.5	33° 59' 50"
8	+20	2.5	33° 59' 40"
9	+20	4.0	33° 59' 30"

B. 320 4F QRM Structure

In order to control Ψ angle to within one degree of accuracy and maintain overall symmetry of the resonator structure, the QRM design was modified to incorporate a crystal blank with 4 precisely ground flats (Fig. 9) that define the mounting locations [8]. This ensured that the determination of Ψ was only dependent on the flat grinding process. The flats were placed at Ψ = -20, 0, and +20° and at 90° increments from the first ground flat as defined by Fig. 10. Finally, a new forming tool with extremely tight tolerances was made to enable the blank to be positioned accurately.

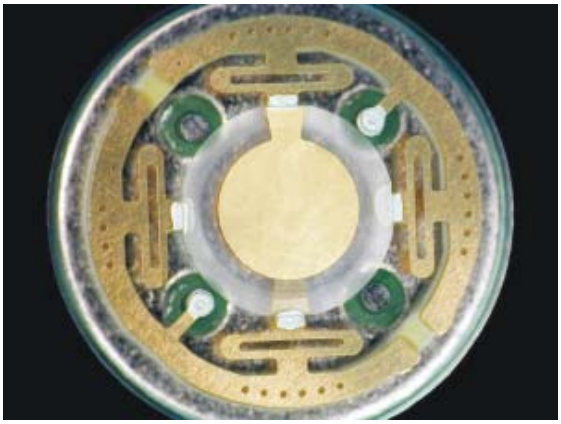

Fig. 9. 320 4F QRM resonator structure.

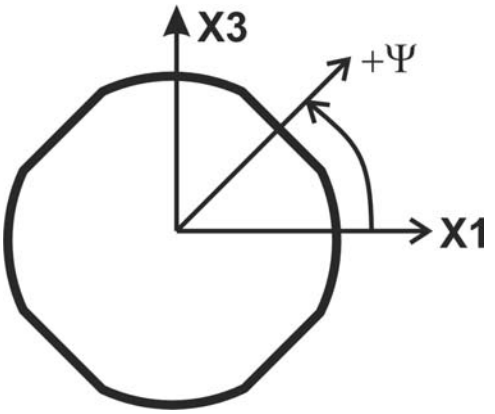

Fig. 10. Definition of Ψ angle for the DOE experiment.

C. Crystal Parameter and G-Sensitivity Results

The average group values for resistance and quality factor are shown in Table III, while the turnover data is shown in Fig. 11. The lowest resistances were achieved by group 7, while the highest Qs were generally achieved by the steeper contours. It is also interesting to note the pattern of decreasing turnover temperature as a function of Ψ for each contour value. It appears that there is an effective angle shift caused by the rotation of Ψ angle, possibly caused by stress effects.

TABLE III
CRYSTAL PARAMETER AVERAGES

Group	Plano-convex 10MHz 3rd overtone 4 flats			
	Contour (diopter)	Ψ angle (°)	Resistance (Ω)	Q-Factor (10^6)
1	1.5	-20	107	0.88
4	1.5	0	94	0.99
7	1.5	+20	88	1.06
2	2.5	-20	98	1.16
5	2.5	0	106	1.08
8	2.5	+20	96	1.17
3	4.0	-20	110	1.24
6	4.0	0	125	1.10
9	4.0	+20	124	1.13

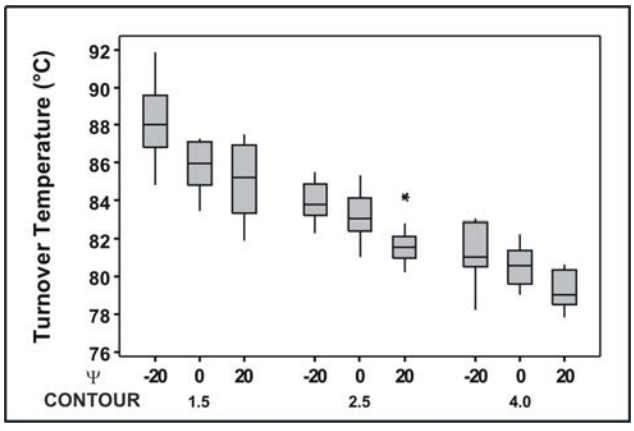

Fig. 11. Turnover temperature results grouped by contour and Ψ angle.

The total Γ g-sensitivity results are shown in Table IV and Fig. 12, while the averages for the components of Γ are shown in Table V. With the exception of the 2.5 diopter contour (coupled modes were evident in those groups), it is obvious that g-sensitvity is very dependent on Ψ angle, with the best mean and sigma values being achieved by groups 7 and 9 for a Ψ of +20°.

Looking at Table V, it is clear that the Γy component is dominant for a Ψ of -20°, while the Γx component becomes dominant for a Ψ of 0°. For a Ψ of +20°, all the components of Γ become fairly balanced and small, with a slight exception for group 8 (2.5 diopter).

TABLE IV
DOE G-SENSITIVITY RESULTS TOTAL Γ

Group	Plano-convex 10MHz 3rd overtone 4 flats					
	Contour (diopter)	Ψ (°)	|Γ| (10^{-9} /g)			
			min	μ	max	σ
1	1.5	-20	0.111	0.185	0.239	0.037
4	1.5	0	0.061	0.159	0.264	0.052
7	1.5	+20	0.029	0.075	0.118	0.026
2	2.5	-20	0.064	0.205	0.353	0.105
5	2.5	0	0.133	0.186	0.263	0.043
8	2.5	+20	0.077	0.190	0.345	0.083
3	4.0	-20	0.096	0.149	0.174	0.024
6	4.0	0	0.161	0.202	0.257	0.031
9	4.0	+20	0.057	0.082	0.105	0.016

TABLE V
DOE G-SENSITIVITY RESULTS Γ COMPONENTS

Group	Plano-convex 10MHz 3rd overtone 4 flats				
	Contour (diopter)	Ψ (°)	Averages Γi (10^{-9} /g)		
			Γx	Γy	Γz
1	1.5	-20	0.068	0.148	0.073
4	1.5	0	0.116	0.041	0.087
7	1.5	+20	0.035	0.042	0.038
2	2.5	-20	0.082	0.129	0.104
5	2.5	0	0.125	0.057	0.112
8	2.5	+20	0.103	0.112	0.079
3	4.0	-20	0.071	0.119	0.042
6	4.0	0	0.169	0.043	0.093
9	4.0	+20	0.054	0.029	0.042

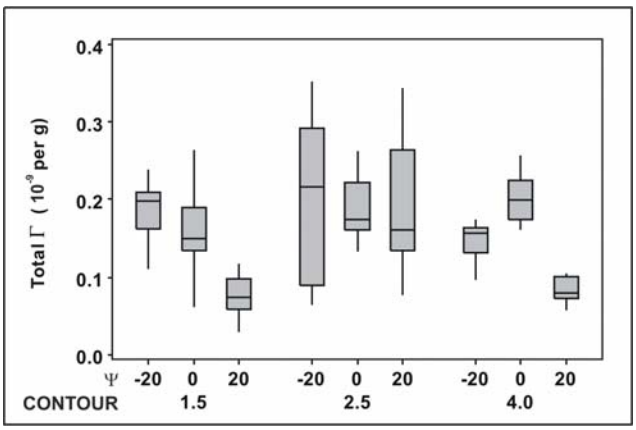

Fig. 12. Total Γ results grouped by contour and Ψ angle.

V. Larger 390 QRM Resonator

Achieving decent crystal parameters with the 320 QRM has been a challenge and appears to be dependent on both Ψ angle and contour. A 0.390" 1.5 diopter version of the QRM resonator (Fig. 13) was designed and built in order to evaluate any enhancement in crystal parameters and to see if we could still achieve low values of g-sensitivity. There was an improvement in the observed resistance and quality factor as shown in Figs. 14 and 15, respectively. Also, the g-sensitivity (Fig. 16) is identical to the 320 QRM for the same contour and Ψ angle. However, the 390 QRM requires formed electrical connections and a standard profile HC40 with nail head pins instead of the low profile package used for the 320 QRM.

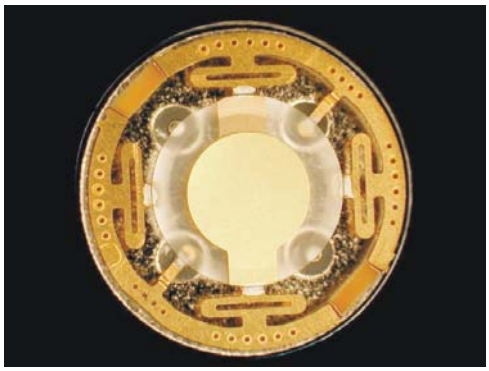

Fig. 13. 390 QRM resonator (ϕ = 23° and Ψ = -20°).

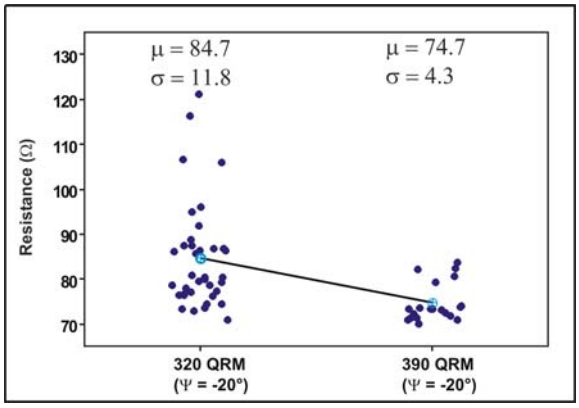

Fig. 14. 390 QRM resistance (ϕ = 23° and Ψ = -20°).

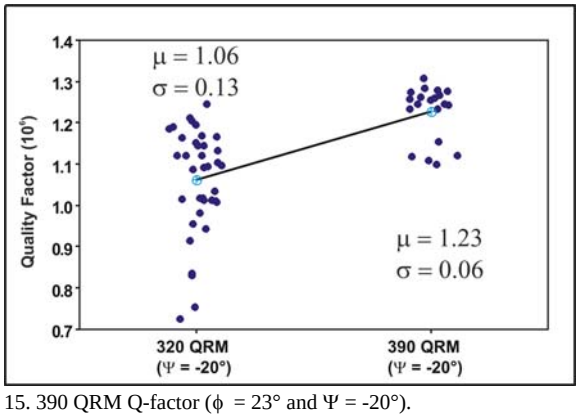

Fig. 15. 390 QRM Q-factor (ϕ = 23° and Ψ = -20°).

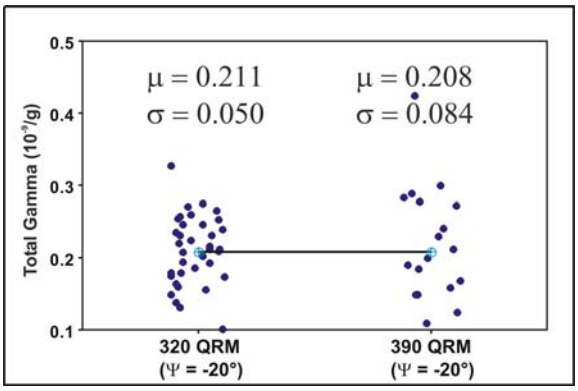

Fig. 16. 390 QRM g-sensitivity (ϕ = 23° and Ψ = -20°).

VI. Conclusions And Future Work

Improvements in the design and manufacture of the QRM resonator have resulted in a robust structure that can be manufactured with precision and reproducibility. An experiment using 0.320" crystal blanks has also shown there is a strong dependence on Ψ angle for achieving low values of g-sensitivity and good crystal parameters. Additionally, preliminary results have shown that a 0.390" version of the QRM resonator performs as well as the 0.320" version for g-sensitivity and better performance is achieved for crystal parameters.

Future work will be focused on refining performance of 320 and 390 QRM structures. This will be done by studying the effects of a narrower range of azimuthal Ψ angle on a variety of crystal cuts (i.e. ϕ = 22, 23, and 24°) to accommodate a wide range of turnover temperatures and applications.

Acknowledgment

The authors would like to thank Al Natale and Bob Raker at VI-Norwalk for performing mechanical resonance measurements and Douglas Shick at NRS Associates LLC for performing the FEA analysis.

Thanks are also given to Karen Messer, Steven Vinson, and Joe Kappes at VI-CINOX for assistance in assembly and documentation and Veer Narayanan at VI-Hudson for assisting with the g-sensitivity measurements.

Additional thanks are given to Errol Eernisse of Quartzdyne for providing force-frequency and mode shape calculations.

References

[1] H.F. Tiersten and Y.S. Zhou, "The increase in the in-plane acceleration sensitivity due to its thickness asymmetry," *Proc. 45th Annual Symposium on Frequency Control*, pp. 289-297, 1991.

[2] H.F. Tiersten and Y.S. Zhou, "An analysis of the in-plane acceleration sensitivity of contoured quartz resonators with rectangular supports," *Proc. 44th Annual Symposium on Frequency Control*, pp. 461-467, 1990.

[3] Y.S. Zhou and H.F. Tiersten, “On the influence of a fabrication imperfection on the normal acceleration sensitivity of contoured quartz resonators with rectangular supports,” *Proc. 44th Annual Symposium on Frequency Control*, pp. 452-460, 1990

[4] R.B. Haskell, P.E. Morley, and D.S. Stevens, “High Q Precision SC cut resonators with low acceleration sensitivity,” *Proc. 56th Annual Symposium on Frequency Control*, pp. 111-118, 2002.

[5] P.E. Morley, R.B. Haskell, and D.S. Stevens, “Low acceleration sensitivity mounting structures for crystal resonators,” *Patent Pending*.

[6] P.E. Morley and R.B. Haskell, “Method for measurement of the sensitivity of crystal resonators to repetitive stimuli,” *Proc. 56th Annual Symposium on Frequency Control*, pp. 61-65, 2002.

[7] J.T. Stewart, P.E. Morley, and D.S. Stevens, “Theoretical and experimental results for the acceleration sensitivity of rectangular crystal resonators,” *Proc. 53rd Annual Symposium on Frequency Control*, pp. 489-493, 1999.

[8] T.J. Lukaszek and A. Ballato, “Resonators for severe environments,” *Proc. 33rd Annual Symposium on Frequency Control*, pp. 311-321, 1979.